
Determination of Stand Properties in Boreal and Temperate Forests Using High-Resolution Imagery

H.H. Shugart, Laura Bourgeau-Chavez, and E.S. Kasischke

ABSTRACT. The existence of a relatively long (ca. 40 yr) satellite imagery archive for examination of potential worldwide forest change motivated an inspection of the relation between forest features observable from higher resolution airborne and satellite imagery and measures of forest biomass, height, and age. Using these data, we inspected the relation between stand age, mean diameter, height, and standing aboveground biomass for forest stands located in boreal forest (near Fairbanks, Alaska) and temperate forest (near Durham, North Carolina). The features of a spatial statistic, semivariance, prove to be related to the structure, age, and biomass patterns of these forests. These initial results indicate the feasibility of using appropriately calibrated high-resolution satellite imagery to estimate and monitor aboveground carbon reserves of forests. *FOR. SCI.* 46(4):478–486.

Additional Key Words: Semivariance, Alaska, North Carolina, remote sensing, biomass.

FORESTERS HAVE LONG HAD AN INTEREST in the estimation of stand height, density, and biomass (volume) from easily obtained observations and have used aerial photographs and satellite images toward this end. Current interests in estimating changes in global, continental, or regional repositories of carbon are a current topical manifestation of this traditional problem. A globally distributed set of high-resolution satellite imagery collected between 1960 and 1972 using classified satellites called the Corona system¹ has recently been declassified by the U.S. government. In addition, high-resolution imagery (~1 m) from commercial satellites is now available. Other data from historical reconnaissance imagery (HRI) are also of high resolution and, combined with the declassified material, provide globally sampled coverage of vegetation over a span of four decades (1960 to the present).

¹ These images and a history of their collection and eventual declassification can be obtained from the National Reconnaissance Office (<http://www.nro.odci.gov/corona.html>). This website also provides a detailed description of the satellites used to collect these data and the other useful information. The US Geological Survey's EROS Data Center archives technical details and sells the images (<http://edcwww.cr.usgs.gov/webglis>) under the product category, "Declassified Intelligence Satellite Photos."

Taken as a whole, this inventory of high-resolution imagery represents a valuable source of archival and current information for determining and monitoring details of 40 yr of ecosystem change. The imagery covers the same time period for which we have direct measurements of changes in the atmospheric pool of CO₂ (e.g., Keeling 1983, Harris and Bodhaine 1983). Thus, there is potential for using this imagery to better quantify changes in biospheric pools of living carbon. Forested regions of the earth play a key role in governing the global carbon budget through interaction with the atmosphere. We are interested in assessing and documenting the capabilities of high-resolution imagery for forest biomass and forest structure quantification and inventory. Our objective in this study is to test the capability of these satellite-based systems with respect to predicting features of forests in two well-studied sites and to compare the results from the aerial photography with the satellite-based systems as a benchmark of their capability. This article represents an initial test of the efficacy of these systems for registering the change in fundamental attributes of forests at different locations.

Herman H. Shugart, Professor, Department of Environmental Sciences, University of Virginia, Charlottesville, VA 22901; Laura L. Bourgeau-Chavez, Research Scientist, ERIM International Inc., P.O. Box 134008, Ann Arbor, MI 48113-4008—Phone: (734) 994-1200, ext. 2897; Fax: (734) 994-5824; E-mail: chavez@erim-int.com; and Eric S. Kasischke, Senior Scientist, ERIM International Inc., P.O. Box 134008, Ann Arbor, MI 48113-4008.

Acknowledgments: This work was conducted under the auspices of MEDEA, a scientific advisory group working with the White House and the National Security Community on environmental issues. The authors would like to thank Dr. L.S. Zall and Dr. R.A. Shuchman for their support and assistance in developing this study. They would also like to thank J.D. Lyden, N.P. Malinas, D.W. Kletzi, and D. Miller for their assistance on the project.

To investigate the potential utility of high-resolution imagery as a basis for a global survey of terrestrial carbon pools, we focused on historical reconnaissance imagery (HRI). These data were used to analyze the relationship between satellite image texture (measured as semivariance) and forest properties at two forest sites, the temperate Duke Forest and the boreal Bonanza Creek Long-Term Ecological Research Site.

Methods

If the spatial heterogeneity of a forest canopy is a reflection of underlying forest processes, then one might expect the spatial statistics of forest canopies to reflect other process-related features such as biomass or forest productivity. One might expect such relationships, in part, because changes in fine-scale textural features of canopies such as the sizes of tree crowns reflect tree growth. Further, at an only slightly larger resolution, the balance of gaps and nongaps in the forest canopy reflects death and recovery of the forest canopy occupied. Both crown growth and gap dynamics are important in the structure, biomass, and productivity processes in natural forests.

Application of Texture Analysis to Forest Problems

High-resolution satellite imagery provides an extensive methodology to assess spatial heterogeneity of forest canopies. An initial problem is to quantify the spatial pattern from the satellite imagery to provide an index of the spatial heterogeneity. Autocorrelation analysis, semivariance analysis, and related statistical techniques (textural analysis techniques) have been widely used to characterize and quantify spatial patterns. Initial applications utilizing the semivariogram were in geology (e.g., Carr 1996, Olea 1994, Elliot 1989) and included topics covering a wide range of spatial scales. Subsequent applications in ecology have focused on the characterization of canopy spatial heterogeneity (Cohen et al. 1990, Ripple et al. 1991, Bradshaw and Spies 1992, Cohen and Spies 1992). For example, Cohen et al. (1990) analyzed the spatial patterns of digital imagery from aerial videography of a chronosequence (80, 140, and 450 yr) of *Pseudotsuga menziesii* stands in the Willamette National Forest in the Cascade Range of western Oregon. Image gray-scale values represented sunlit crowns and shadow patterns formed by discontinuities of canopy features. These patterns resulted from sun-angle geometry and biological factors (e.g., tree height, canopy dimensions, and gap-dynamics) and

were highly correlated to stand age and tree size variability (Cohen and Spies 1992).

The actual mathematics used to create a semivariogram from a data set have varied slightly from application to application and from author to author (e.g., Cohen et al. 1990, St-Onge and Cavayas 1997). However, a semivariogram can basically be described as an autocorrelation (correlogram) technique. In fact, the two functions (semivariance and autocorrelation) are inversely related through their similar basis in spatial covariance (Cressie 1991, Isaaks and Srivastava 1989). The semivariogram characterizes the distribution of a regionalized variable (variable whose position in space or time is known), just as the statistical variance describes the distribution of a nonspatial random variable (Woodcock 1987). The distance at which data samples become independent or decorrelated is called the "range." The sill is defined as the variance value where the semivariogram levels off. It should be noted that if a well-defined structure occurs in one direction, such as row plantings, one would expect the variance to oscillate around the sill.

Site Selection

The boreal site chosen for this study was located at the Bonanza Creek Experimental Forest near Fairbanks, Alaska (64°42.5'N 148°15.0'W) and consisted of black spruce (*Picea mariana* [Moench] Voss) and white spruce (*Picea glauca* [Mill] B.S.P.) stands. These forest types are similar in canopy architecture and dominate Alaska's boreal forest as well as much of the Canadian boreal forest. The temperate site was Duke Forest in Durham, North Carolina (36°N 79°W). Duke Forest stands consisted of loblolly pine (*Pinus taeda*), a typical southern pine forest type. The Duke Forest and Bonanza Creek sites were selected because of their long-term ecological studies. The stands chosen from the Duke Forest test site are representative of a successional chronosequence. Those from Bonanza Creek represent various densities and biomass levels. Stand measurements collected at Duke Forest included average tree diameter, stand density, stand biomass, and stand age (Table 1). For a more detailed description of stand variables and data collection methods see Kasischke (1992) or Kasischke et al. (1994). Measurements collected at Bonanza Creek included average tree height, average tree diameter, stand density, and stand biomass (Table 2). These data were archived on a CD-ROM by the Jet Propulsion Laboratory as part of their studies at this research area (Way et al. 1992).

Table 1. Forest parameters measured at Duke Forest and semivariance statistics for the historical reconnaissance imagery.

Forest type	Stand age (yr)	Stand density (stems/ha)	Average tree diameter (cm)	Stand biomass (m ton/ha)	Aerial photography		HRI data	
					1/e lag distance (pixels)	Normalized variance	1/e lag distance (pixels)	Normalized variance
Loblolly pine plantation	2	14,939	1.9	1.5	2.5	0.015	2.5	0.004
Loblolly pine plantation	8	11,634	8.5	88.3	2.5	0.046	3.0	0.009
Loblolly pine plantation	25	1,583	21.5	329.0	2.0	0.030	4.0	0.009
Loblolly pine plantation	40	200	31.1	130.0	3.0	0.074	5.0	0.012
Loblolly pine plantation	60	310	38.1	350.0	3.0	0.074	6.5	0.010
Loblolly pine plantation	90	190	43.0	250.0	3.5	0.046	8.0	0.013

Table 2. Forest parameters measured at Bonanza Creek and semivariance statistics for the historical reconnaissance imagery.

Forest type and stand number	Stand density (stems/ha)	Average tree diameter (cm)	Average tree height (m)	Stand biomass (m ton/ha)	1/e lag distance (pixels)	Normalized variance
Black spruce—01a	1,975	8.8	7.6	37.0	3.5	0.077
Black spruce—01b	1,975	8.8	7.6	37.0	3.0	0.035
Black spruce—02	1,402	8.2	6.8	23.1	3.0	0.043
White spruce—01	1,248	19.6	22.1	216.9	3.5	0.192
White spruce—02	2,073	14.5	20.1	167.1	3.5	0.147
White spruce—04	608	25.0	22.0	163.3	4.0	0.169
White spruce—05	1,484	17.9	21.3	181.3	4.0	0.199
White spruce—19	1,564	16.6	missing	172.0	4.0	0.181
White spruce—23	1,135	13.9	12.3	60.3	4.5	0.071

Photos of the three ecosystem types are presented in Figure 1. Note the low stature of the black spruce stand in Figure 1A. The white spruce stand (Figure 1B) has similar canopy architecture, but the trees are much larger. While the canopy width is somewhat greater, the white spruce have the narrow conical shape similar to black spruce. The trees in the loblolly pine stand shown in Figure 1C are not only taller, but the canopy width is much greater than in the boreal forest. Also the lower dead branches are shed from the loblolly such that the canopy depth is relatively shallow in relation to tree height. This is in contrast to the spruce trees that retain their lower dead branches. Beneath the loblolly canopy is a devel-

oping understory of hardwood species reflecting the typical successional pattern of loblolly pine.

Although coniferous trees dominate the boreal and temperate test sites, they represent distinctly different forest types with completely different canopy geometry and successional patterns. While loblolly pine is an early successional species that is typically replaced by broad-leaved deciduous trees, white spruce is a late successional species (with successional antecedent broad-leaved species), and black spruce is often self-perpetuated by wildfire. The canopy structure is much simpler in the boreal sites, which possess fewer vertical layers than temperate pine forests. Generally, stand density in



A



B



C

Figure 1. (A) Ground photograph of mature black spruce stand from Bonanza Creek, Alaska. (B) Ground photograph of mature white spruce stand from Bonanza Creek, Alaska. (C) Ground photograph of mature loblolly pine forests of Duke Forest, North Carolina.

boreal spruce stands decreases as the canopy closes in middle stages of development. In later stages, gaps develop in the canopy, and density decreases further. White spruce will regenerate in its own shade and may take advantage of gaps in the canopy, but black spruce cannot. In the absence of fire, black spruce ecosystems eventually begin to degrade as the soils become shallower and colder, moss grows thicker, trees die, and the overall environment becomes unfavorable for seed regeneration.

Semivariance Technique

Semivariance (γ) was calculated using the expression:

$$\gamma(\mathbf{x}) = C(0) - C(\mathbf{x}) \quad (1)$$

where $C(\mathbf{x})$ represents the value of the autocovariance function at location \mathbf{x} . In our case, \mathbf{x} represents a location in two-dimensional space. $C(0)$ represents the autocovariance function at the origin which is also representative of the overall variance of the image. The autocovariance function was calculated using Fourier techniques (Oppenheim and Schaffer 1989). As described in that text, the autocovariance of a signal can be calculated by taking the inverse Fourier transform of the signal's power spectrum. When performing this process using the Fast Fourier Transform (FFT), care must be taken to avoid aliasing or "wrap-around" effects. These effects can be avoided by simply broadening the extent of the signal passed through the FFT by zero-padding. For a complete description of the theory of Fourier Analysis and its application to autocovariance, see Oppenheim and Schaffer (1989).

The semivariance technique used in this study is based on a sampling of image pixels. Semivariograms were generated for the image subsets using the following steps:

1. All image chips were square, with n pixels on a side.
2. The image chip intensity was normalized to unit mean to remove any differences due to overall brightness.
3. The mean intensity was subtracted so that the Fourier process below calculates the autocovariance function rather than the autocorrelation function.
4. The spatial extent of the image chip was zero-padded to $2n \times 2n$ pixels to avoid aliasing artifacts.
5. The image chip spectrum was calculated using the FFT.
6. The power spectrum of the image chip was calculated by multiplying each spectral value by its complex conjugate.
7. The autocovariance function was calculated by applying the inverse FFT to the power spectrum and dividing the resultant image by n^2 , the number of points in the original image chip.
8. The value of the semivariance at each point \mathbf{x} was calculated by subtracting the value of the autocovariance function at \mathbf{x} from the value of the autocovariance function at the origin, as per Equation (1).

The descriptive statistics derived from the semivariograms were normalized variance and lag distance. Variance was normalized to allow between scene comparisons. The data were also normalized such that any sized subsets can be compared. The lag was defined as the distance where the semivariogram reaches a value equal to $(1 - 1/e)$ of its maximum. This is a standard measure of lag distance used in

autocorrelation (Oppenheim and Schaffer 1989). The " $1/e$ " lag was calculated in two dimensions because the procedure produces a two-dimensional semivariogram. The two lags were then averaged. It should be noted that averaging is not acceptable if a well-defined structure occurs in one direction and not the other (anisotropy), since lags will differ greatly. The technique used in this article for calculation of semivariance assumes the data are isotropic. A comparison was made of two-dimensional semivariograms from several directions within each image chip to check for isotropy. These comparisons did not show any indication of anisotropy in the data.

Remote Sensing Methods

In our analysis, we used semivariance techniques on historical reconnaissance imagery (HRI) from Bonanza Creek and Duke Forest, as well as on a digital orthophoto quadrangle (digital aerial photograph) of Duke Forest. The digital aerial photograph of Duke Forest is used to provide a detailed example of the semivariance technique used for both the aerial photo and HRI analyses. The Duke HRI data were from April 1994 and the Bonanza Creek data were from August 1993. The sensor used in this analysis is a camera system collecting data in the visible region of the electromagnetic spectrum. The data were provided to us in digital form. The processing of the visible imagery was performed on the gray scale values as provided. Although we are not at liberty to reveal the finest resolution of the imagery used in this analysis, it was sufficiently fine to accurately measure the lags of the correlations. This is not to say that coarser resolution imagery is not useful for measuring lags, it is useful for measuring structures of coarser scales. The aerial photograph was collected in March 1993 (Figure 2) and digitized by USGS with 1 m resolution. Subsets of the various test stands were extracted from all three images for analysis. The same techniques as described below for the aerial photograph were used for the HRI data.

The subsets of the various aged Duke Forest stands (Figure 3) extracted from the digital data for semivariance analysis were between 82 and 124 pixels on a side. Subsets were made as large as possible while remaining within stand boundaries and avoiding stand edges. Semivariograms were computed for each image subset using the technique described above. The actual image subsets used in the analysis are presented with the corresponding semivariograms in Figure 3. The $1/e$ lag distance and maximum variance (normalized variance) were calculated from each semivariogram. To examine relationships between these variables and stand structure, simple linear regression analyses were performed with $1/e$ lag distance and normalized variance as independent variables and the various forest parameters as dependent variables (listed in Tables 1 and 2).

Results

Duke Forest Digital Aerial Photograph Results

Textural differences between various aged forest stands are apparent in the image subsets and semivariograms of Figure 3. Further, there is a noticeable lack of directional

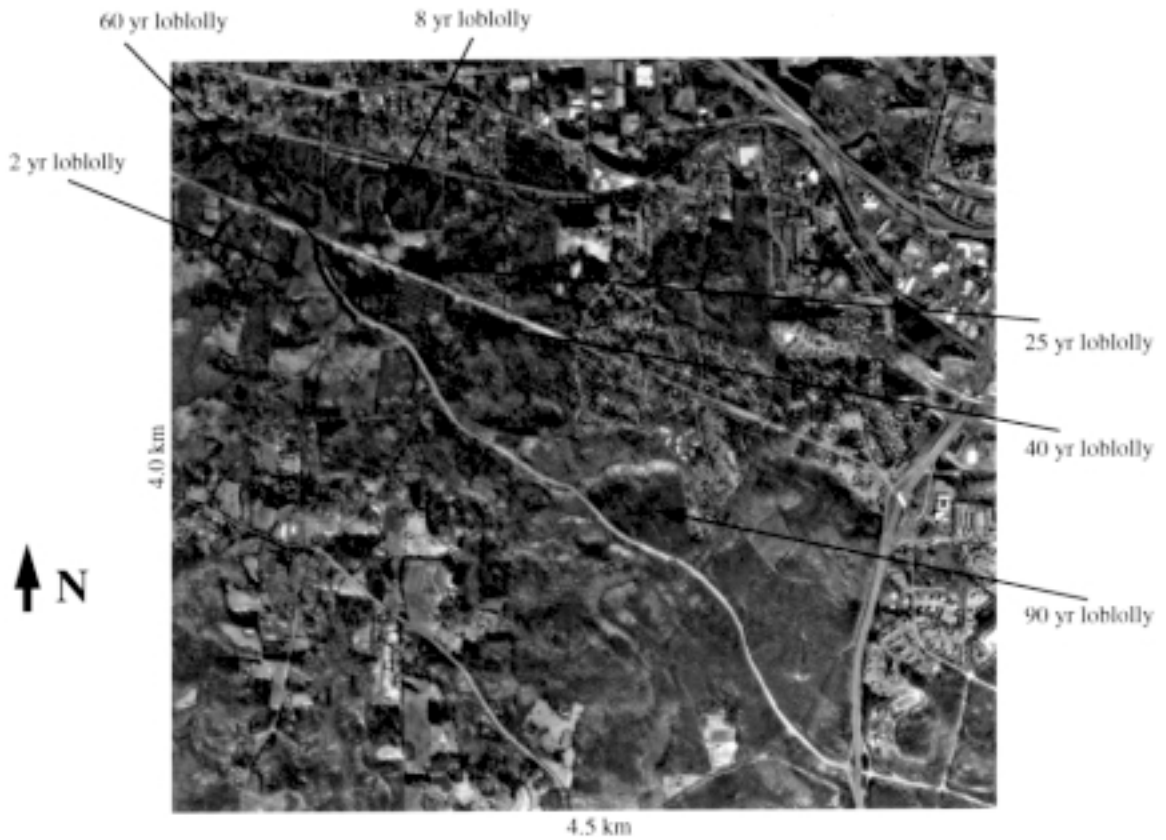


Figure 2. Digital aerial photograph of Duke Forest with loblolly test sites labeled.

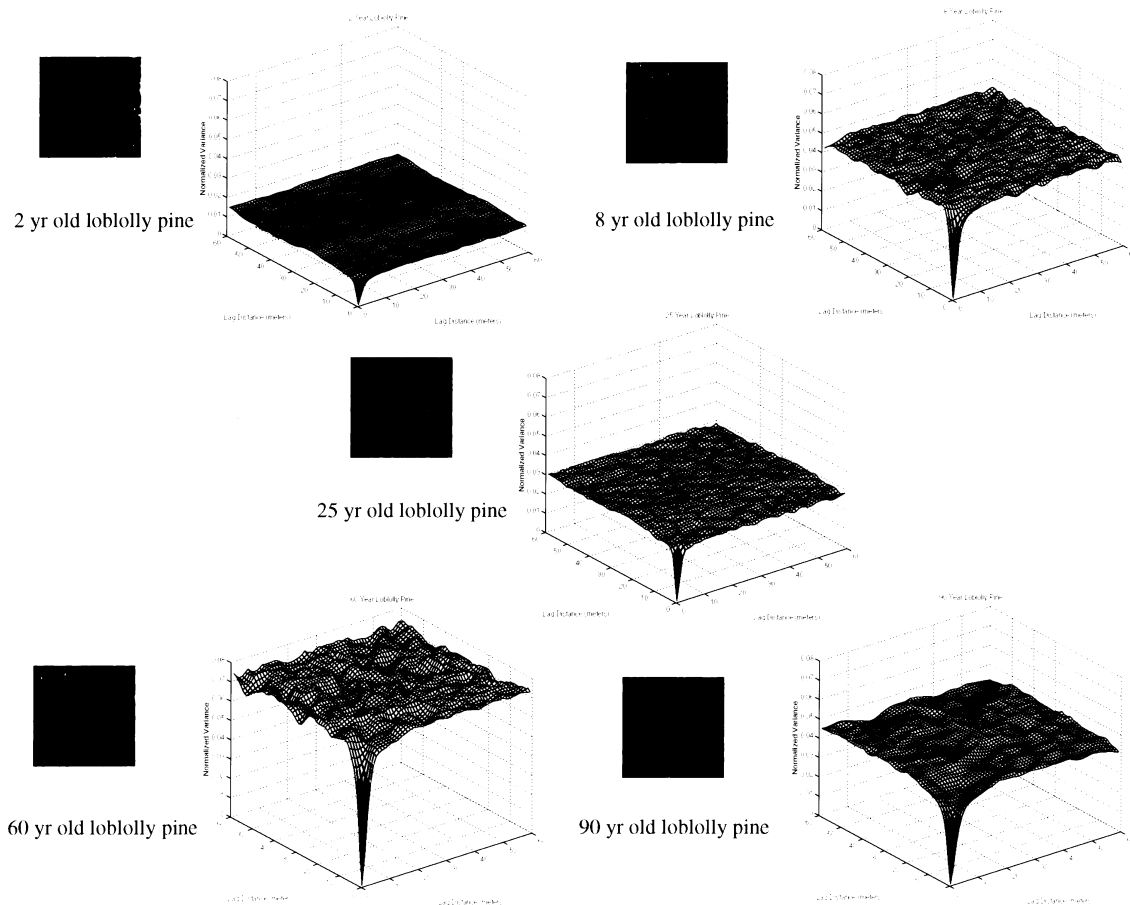


Figure 3. Three-dimensional semivariogram plots for Duke Forest test sites with corresponding aerial photograph image subsets.

dependence (anisotropy) in the semivariograms. Greater clumping and variation in the forest canopy leads to increased lag distances and higher sills (variance) in the semivariograms. The lag is representative of the canopy or gap sizes and the normalized variance of the number of gaps. A two-dimensional comparison of semivariograms (using lag distance in one direction) from all stands revealed distinct differences in normalized variance and lag among the various aged pine stands (Figure 4a).

A correlation (r) analysis of lag distance and normalized variance versus stand parameters was conducted for all loblolly sites (Table 3). The scatter plot of diameter and normalized variance shows a positive linear association while the scatter plot of density and normalized variance shows a negative linear association. Although the normalized variance was moderately correlated with mean stand diameter and stand density, the P -values showed the relationships to be insignificant at the 5% level. The $1/e$ lag distance was found to most strongly correlate with stand age (0.815) and secondarily with mean diameter (0.717). However, the latter correlation was significant only to 11%.

The simple linear regression of $1/e$ lag on forest age (Table 4) has a coefficient of determination (R^2) of 0.665, standard

error (SE) of 21.58, and P -value of 0.048. This regression equation meets all model assumptions including normality, homogeneity, and independent observations.

Duke Forest Historical Reconnaissance Imagery Results

A comparison of the two-dimensional semivariogram plots from Duke HRI data (Figure 4b) to the aerial photograph-based plots (Figure 4a) show that the sills are not directly related to forest age; however, they appear to be more so for the HRI data than the aerial photograph. Scatterplots of normalized variance versus stand age for both the aerial photograph and HRI data show the relationships to be curvilinear. For the HRI data, the correlation of the square of normalized variance on age has a correlation coefficient of 0.838 and a P -value of 0.037. However, the equivalent scatter plot and correlation ($r = 0.44$, P -value = 0.38) for the aerial photograph show the relationship to be insignificant. Table 3 presents the correlation coefficients (r) for all stand parameters versus semivariogram variables for the HRI data. All correlations are quite high (0.80 to 0.998) except those with stand biomass (0.543 and 0.647). The best correlation, as with the aerial photograph

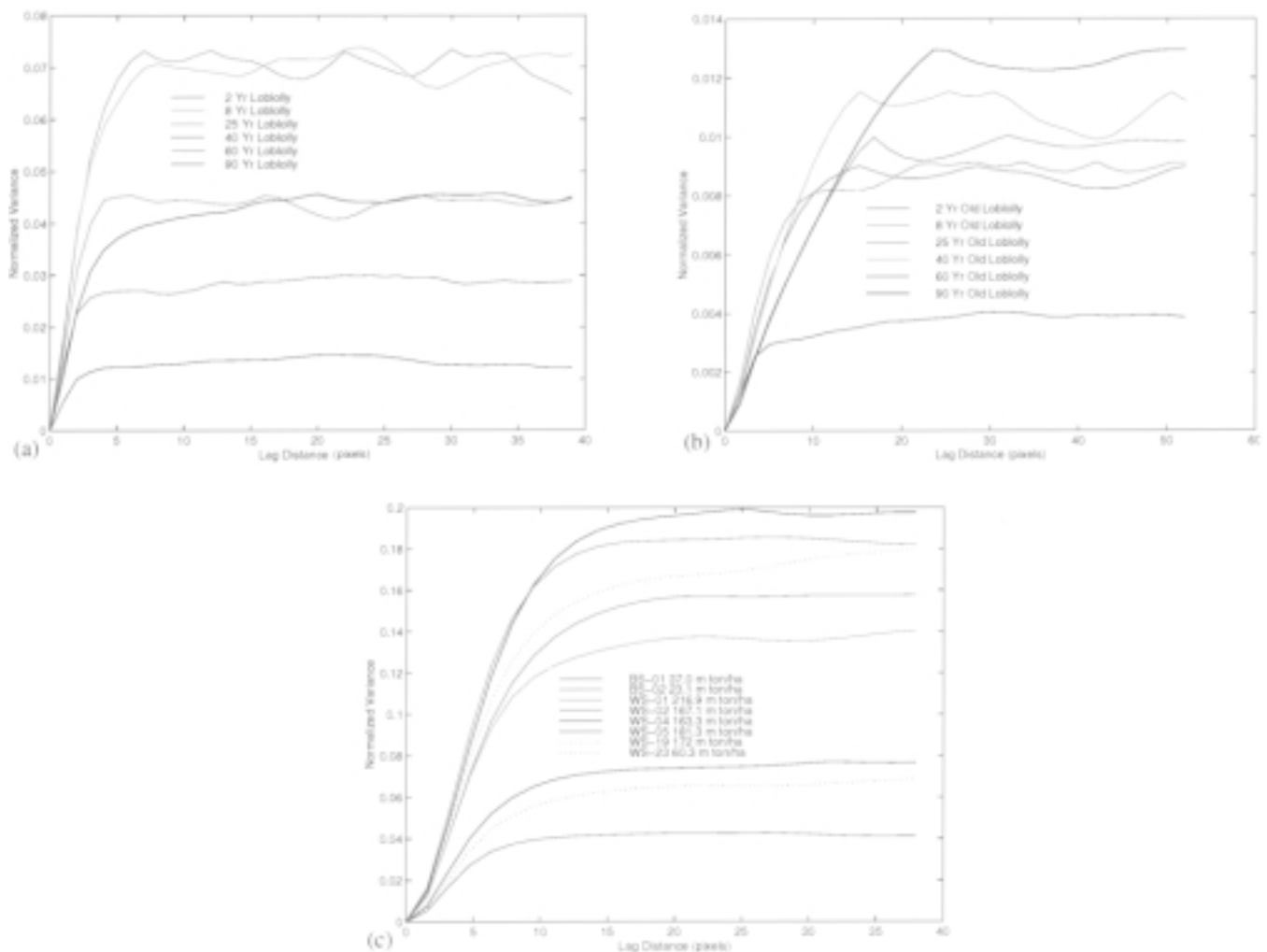


Figure 4. (A) Aerial photograph two-dimensional semivariogram plots for Duke Forest test sites. (B) Historical reconnaissance imagery two-dimensional semivariogram plots for Duke Forest test sites. (C) Historical reconnaissance imagery two-dimensional semivariogram plots for Bonanza Creek test sites.

Table 3. Pearson correlation coefficients for all stand variables measured for the Duke Forest and Bonanza Creek forest sites and semivariance summary statistics.

Location and stand attribute	Pearson correlation coefficients with normalized variance		Pearson correlation coefficients with 1/e lag distance	
Duke Forest				
(aerial photograph)				
Stand age (<i>n</i> = 6)	+0.512	<i>P</i> -value = 0.302	+0.815	<i>P</i> -value = 0.0481
Mean stand diameter (<i>n</i> = 6)	+0.685	<i>P</i> -value = 0.135	+0.717	<i>P</i> -value = 0.109
Stand density (<i>n</i> = 6)	-0.662	<i>P</i> -value = 0.155	-0.432	<i>P</i> -value = 0.392
Stand biomass (<i>n</i> = 6)	+0.395	<i>P</i> -value = 0.446	+0.104	<i>P</i> -value = 0.844
Duke Forest				
(historical reconnaissance imagery)				
Stand age (<i>n</i> = 6)	+0.807	<i>P</i> -value = 0.058	+0.998	<i>P</i> -value = 0.000007
Mean stand diameter (<i>n</i> = 6)	+0.856	<i>P</i> -value = 0.028	+0.963	<i>P</i> -value = 0.002
Stand density (<i>n</i> = 6)	-0.817	<i>P</i> -value = 0.039	-0.800	<i>P</i> -value = 0.056
Stand biomass (<i>n</i> = 6)	+0.543	<i>P</i> -value = 0.284	+0.647	<i>P</i> -value = 0.165
Bonanza Creek Forest				
(historical reconnaissance imagery)				
Stand height (<i>n</i> = 8)	+0.959	<i>P</i> -value = 0.0002	+0.460	<i>P</i> -value = 0.251
Mean stand diameter (<i>n</i> = 9)	+0.832	<i>P</i> -value = 0.005	+0.571	<i>P</i> -value = 0.108
Stand density (<i>n</i> = 9)	-0.311	<i>P</i> -value = 0.411	-0.513	<i>P</i> -value = 0.158
Stand biomass (<i>n</i> = 9)	+0.969	<i>P</i> -value = 0.00002	+0.367	<i>P</i> -value = 0.331

analysis, was between 1/e lag distance and stand age (0.998).

The simple linear regression of forest stand age versus 1/e lag distance (Table 4) has a coefficient of determination (R^2) of 0.996, standard error of 2.41 and *P*-value of 0.000007. The analogous regression of diameter on 1/e lag distance has a coefficient of determination of 0.927 with a standard error of 4.94 and *P*-value of 0.002. Both of these regression equations are significant and meet all model assumptions. A regression of the square of normalized variance versus stand age resulted in a significant linear relationship with an R^2 of 0.702, *P*-value of 0.037, and SE of 20.33. The stand age-1/e lag distance regression proved to be a better all-around model.

The regression of normalized variance on stand density had an R^2 of 0.695 and *P*-value of 0.039, but the standard error was high, 4120.6. A plot of estimated density versus measured density showed the model to be strongly overestimating or underestimating stand density. It was determined

to be a poor model, and therefore it is not presented in Table 4. The regression of normalized variance on average diameter was significant with a strong coefficient of determination, but it was not as good as the model of 1/e lag distance on diameter. The normalized variance model had a lower coefficient of determination (0.739 vs. 0.927), higher standard error (9.37 vs. 4.94), and higher *P*-value (0.028 vs. 0.002). It should be noted that the Duke analysis, while highly significant, is based on a small sample size, thus caution must be taken in forming any conclusions.

Bonanza Creek Historical Reconnaissance Imagery Results

A fairly strong relationship between normalized variance (sills) and forest biomass is apparent from the two-dimensional semivariogram plots (Figure 4c). This relationship is reflected in the correlation coefficient for these two variables ($r = 0.969$). Correlation coefficients for all stand parameters

Table 4. Simple linear regressions for stand variables measured at the Duke Forest and Bonanza Creek sites and semivariance summary statistics. Only regressions that are significant at the 0.05 level with acceptable standard errors are presented.

Location and stand attribute (<i>y</i>)	Significant linear regressions at the 0.05 level with <i>x</i> , the normalized variance (R^2 shown in parentheses)	Significant linear regressions at the 0.05 level with <i>x</i> , the 1/e lag distance (R^2 shown in parentheses)
Duke Forest		
(aerial photograph)		
Stand age (<i>n</i> = 6)		$y = -105 + 51.82x$ ($R^2 = 0.665$)
Duke Forest		
(historical reconnaissance imagery)		
Stand age (<i>n</i> = 6)	$y = -13.67 + 519482.77x^2$ ($R^2 = 0.702$)	$y = -38.57 + 15.739x$ ($R^2 = 0.996$)
Mean stand diameter (<i>n</i> = 6)	$y = -18.561 + 4481.82x$ ($R^2 = 0.739$)	$y = -12.107 + 7.47x$ ($R^2 = 0.927$)
Bonanza Creek Forest		
(historical reconnaissance imagery)		
Stand height (<i>n</i> = 8)	$y = 3.26 + 100.409x$ ($R^2 = 0.919$)	
Mean stand diameter (<i>n</i> = 9)	$y = 6.065 + 70.656x$ ($R^2 = 0.692$)	
Stand biomass (<i>n</i> = 9)	$y = -19.895 + 1110.461x$ ($R^2 = 0.939$)	

and semivariance parameters are presented in Table 3. Note that the height parameter was unavailable for one of the white spruce stands so the correlations are based on 8 rather than 9 cases. The best correlations were between normalized variance and stand biomass and height (0.969 and 0.959, respectively). This is in contrast to the best correlations for Duke forest data sets, which were with $1/e$ lag distance. This is likely due to differences in the structure of the boreal forests in comparison to temperate forests. Also, the correlations between Duke forest biomass and semivariogram parameters were weaker and insignificant when compared to the correlation found between forest biomass and normalized variance in the Bonanza Creek forest.

Regressions of forest biomass, height, and diameter versus normalized variance for the Bonanza Creek stands were all significant and met the assumptions of the model (Table 4). The linear regression between forest biomass and normalized variance had a coefficient of determination of 0.939, SE of 19.94, and P -value of 0.000015; the regression of stand height versus normalized variance had a coefficient of determination of 0.919, SE of 2.15, and P -value of 0.00016; and the regression of mean stand diameter versus normalized variance had a coefficient of determination of 0.692, SE of 3.36, and P -value of 0.0055.

Discussion

Our initial interest in evaluating the utility of textural analysis was to develop a preliminary assessment of the capability of historical reconnaissance imagery to assess differences in forest structure, and our results are promising in this regard. The fidelity in relating stand parameters to normalized variance and $1/e$ lag distance is high (high correlations; large r and R^2 values). Several relationships are significant in a statistical sense, even with the relatively small number of test sites that we used.

Albeit drawn from a small number of samples, the implication of our findings is logically consistent. The fact that normalized variance was a better predictor of stand variables in the boreal zone and $1/e$ lag distance was better for temperate forests is logical given the structural characteristics of these forests and changes that occur to them during succession. Normalized variance and $1/e$ lag distance measure somewhat different aspects of stand structure. The $1/e$ lag distance statistic is an indicator of the typical canopy size in a given forest, while normalized variance tends to index the overall pattern of forest canopies and gaps. Normalized variance corresponds with the importance of density and spacing as controlling factors of standing biomass in boreal spruce forests. Canopy size often does not vary greatly among different aged boreal spruce forests, but tree spacing does. The $1/e$ lag distance has greater value in predicting stand structure in the more closed temperate forests where tree crown dimension varies more widely and where canopy size is an indicator of level of biomass.

The utility of texture analysis is not limited to boreal and temperate zones nor is it limited to coniferous species or even to visible data. Levesque and King (1999) found strong

relations between image semivariance parameters from an airborne digital camera (0.25 to 1.0 m resolution) and forest structure (percent canopy closure, stem density, crown size, tree height) in a broadleaf forest (*Populus tremuloides*) of Ontario. An initial analysis of applying our semivariance techniques to HRI data collected over a tropical test site revealed general trends of increasing variance and lag distance with increasing forest succession (age). The texture analysis allows a means of differentiating the multilayered canopies of mature tropical rainforests from the more closed secondary growth rainforests. Semivariograms showed distinct variances and lag distances for harvested, secondary, and mature rainforests. Luckman et al. (1994) also found texture analysis of imagery to be useful for discriminating forest age in a tropical region. However, their study relied upon C-band Synthetic Aperture Radar (SAR) data. They used the Grey-Level Co-Occurrence Matrix contrast texture technique, which is similar to a 2-D autocorrelation, to discriminate virgin forest from secondary regrowth and clearcut areas.

The methods explored in this paper have potential application as a computational algorithm for digital imagery. Such an application invites the possibility of a regular automated survey of forest reserves, which could enrich the tools available to estimate carbon storage and release from the world's forests. St.-Onge and Cavayas (1997) explored methods of automated forest structure mapping from high-resolution imagery. Their methods involved multidirectional semivariogram calculations and a simple region growing algorithm to delineate and characterize forests of Petawawa National Forest in Ontario, Canada. They concluded that, with the support of GIS data, automated detailed mapping of forests will be feasible in the near future. For this extended application, however, there is an obvious need for calibrated data. Calibration issues are beyond the scope of this study, but they will need to be resolved before worldwide forest surveys may be conducted.

Natural or anthropogenic changes in the carbon pools of boreal forests (primarily through wildfire), temperate forests (primarily through harvesting), and tropical forests (through harvesting and fire) have noted effects on the global carbon budget and possible links to global warming (Pastor and Post 1988, Gates 1990, Schneider 1989, Bonan et al. 1990, Botkin and Simpson 1990). To understand the magnitude and significance of change as well as to balance the carbon budget, it is important to be able to quantify the status of these major carbon pools through time.

It appears that the combination of high-resolution imagery and textural analysis techniques can contribute to the task of monitoring biomass/carbon changes in forest ecosystems. The test sites that we chose are representative of major carbon pools within their respective biomes. Although our sample sizes were small, the results of this analysis demonstrate the strong capabilities of high-resolution imagery for textural analysis and the derivation of forest structure. For future work, we suggest that this technique be applied not only to larger sample sizes but also to other forest types to test its robustness and global utility.

Literature Cited

- BONAN, G.B., H.H. SHUGART, AND D.L. URBAN. 1990. The sensitivity of some high-latitude boreal forests to climatic parameters. *Clim. Change* 16:9–29.
- BOTKIN, D.B., AND L.G. SIMPSON. 1990. Biomass of the North American boreal forest. *Biogeochemistry* 9:161–174.
- BRADSHAW, G.G., AND T.A. SPIES. 1992. Characterizing canopy gap structure in forests using wavelet analysis. *J. Ecol.* 80:205–215.
- CARR, J.R. 1996. Spectral and textural classification of single and multiple band digital images. *Comp. Geosci.* 22:849–865.
- COHEN, W.B., AND T.A. SPIES. 1992. Estimating structural attributes of Douglas-fir/western hemlock forests stands from Landsat and SPOT imagery. *Remote Sens. Environ.* 41:1–17.
- COHEN, W.B., T.A. SPIES, AND G.A. BRADSHAW. 1990. Semivariograms of digital imagery for analysis of conifer canopy structure. *Remote Sens. Environ.* 34:167–178.
- CRESSIE, N.A.C. 1991 *Statistics for spatial data*. Wiley, New York.
- ELLIOT, J.K. 1989. An investigation of the change in surface roughness through time on the foreland of Austre Okstindbreen, North Norway. *Comput. Geosci.* 15:209–217.
- GATES, D.M. 1990. Climate change and the response of forests. *Internat. J. Remote Sens.* 11:1095–1107.
- HARRIS, J.M., AND B.A. BODHAINE (EDS.). 1983. Summary Report 1982, Geophysical monitoring for climatic change. *Environ. Res. Laboratories/NOAA, U.S. Dep. of Comm.*, Washington, DC.
- ISAAKS, E.H., AND R.M. SRIVASTAVA. 1989. *Applied geostatistics*. Oxford University Press, New York.
- KASISCHKE, E.S., CHRISTENSEN, N.L., JR., AND E. HANEY. 1994. Modeling of geometric properties of loblolly pine tree and stand characteristics for use in radar backscatter models, *IEEE Trans. Geosci. Remote Sens.* 32:800–822.
- KASISCHKE, E.S. 1992. Monitoring changes in aboveground biomass in loblolly pine forests multichannel synthetic aperture radar data. Ph.D. Diss., Univ. of Michigan, Ann Arbor, MI.
- KEELING, C.D. 1983. The global carbon cycle: What we know and could know from atmospheric, biospheric and oceanic observations. P. II.3–II.62 in *Proc. of the CO₂ research conference: Carbon dioxide, science, and consensus*. DOE CONF-820970. NTIS, Springfield, VA.
- LEVESQUE, J., AND D.J. KING. 1999. Airborne digital camera image semivariance for evaluation of forest structural damage at an acid mine site. *Remote Sens. Environ.* 68:112–124.
- LUCKMAN, A., G. GROOM, AND J. BAKER. 1994. Forest age discrimination from texture measures of SAR imagery. P. 104–112 in *Proc. of IGARSS'94, Surface and atmospheric remote sensing: Technologies, data analysis, and interpretation*. Vol. I. IEEE 94CH3378-7.
- OLEA, R.A. 1994. Fundamentals of semivariogram estimation modeling and usage. P. 27–35 in *Stochastic modeling and geostatistics: Principles, methods and case studies*, Yarus, J.M., and R.L. Chambers (eds.). AAPG Computer Applications in Geology. Vol 3. Am. Assoc. of Petroleum Geol., Tulsa, Oklahoma.
- OPPENHEIM, A.V., AND R.W. SCHAFFER. 1989. *Discrete-time signal processing*. Prentice-Hall, Englewood Cliffs, NJ.
- PASTOR, J., AND W.M. POST. 1988. Response of northern forests to CO₂-induced climate change. *Nature* 334:55–58.
- RIGNOT, E., J.B. WAY, C. WILLIAMS, AND L. VIREECK. 1994. Radar estimates of aboveground biomass in boreal forests of interior Alaska. *IEEE Trans. Geosci. Rem. Sens.* 32:1117–1124.
- RIPPLE, W.J., G.A. BRADSHAW, AND T.A. SPIES. 1991. Measuring forest landscape patterns in the Cascade Range of Oregon, USA. *Biol. Conserv.* 57:73–88.
- SCHNEIDER, S.H. 1989. The changing climate. *Scien. Am.* 261:70–79.
- ST-ONGE, B.A., AND F. CAVAYAS. 1997. Automated forest structure mapping from high-resolution imagery based on directional semivariogram estimates. *Remote Sens. Environ.* 61:82–95.
- WAY, J.B., ET AL. 1992. Collected data of the Bonanza Creek Experimental Forest, Alaska, Vols. I and II, Version 1 (CD-ROM). Jet Propulsion Lab., Calif. Inst. of Tech., Pasadena, CA.
- WOODCOCK, C. 1987. Spatial analysis of forest images. *Proc. of the First International Workshop on Remote Sensing and Resource Exploration*. ICTP.